RESEARCH PAPER

# Xyloglucan endotransglucosylase-hydrolase30 negatively affects salt tolerance in Arabidopsis

Jingwei Yan[1], Yun Huang[1], Huan He[1], Tong Han[1], Pengcheng Di[1], Julien Sechet[2], Lin Fang[3], Yan Liang[2], Henrik Vibe Scheller[2], Jenny C. Mortimer[2], Lan Ni[1], Mingyi Jiang[1,4], Xilin Hou[4,5] and Aying Zhang[1,4,*,]

[1] College of Life Sciences, Nanjing Agricultural University, Nanjing, Jiangsu, 210095, China

[2] Joint Bioenergy Institute and Environmental Genomics and Systems Biology Division, Lawrence Berkeley National Laboratory, Berkeley, CA 94720, USA

[3] Guangdong Provincial Key Laboratory of Applied Botany, South China Botanical Garden, Chinese Academy of Sciences, Guangzhou 510650, China

[4] State Key Laboratory of Crop Genetics and Germplasm Enhancement, Nanjing Agricultural University, Nanjing, Jiangsu, 210095, China

[5] Key Laboratory of Biology and Germplasm Enhancement of Horticultural Crops in East China, Ministry of Agriculture, Nanjing Agricultural University, Nanjing, Jiangsu, 210095, China

* Correspondence: ayzhang@njau.edu.cn

## Abstract

**Plants have evolved various strategies to sense and respond to saline environments, which severely reduce plant growth and limit agricultural productivity. Alteration to the cell wall is one strategy that helps plants adapt to salt stress. However, the physiological mechanism of how the cell wall components respond to salt stress is not fully understood. Here, we show that expression of *XTH30*, encoding xyloglucan endotransglucosylase-hydrolase30, is strongly up-regulated in response to salt stress in Arabidopsis. Loss-of-function of *XTH30* leads to increased salt tolerance and overexpression of *XTH30* results in salt hypersensitivity. XTH30 is located in the plasma membrane and is highly expressed in the root, flower, stem, and etiolated hypocotyl. The NaCl-induced increase in xyloglucan (XyG)-derived oligosaccharide (XLFG) of the wild type is partly blocked in *xth30* mutants. Loss-of-function of *XTH30* slows down the decrease of crystalline cellulose content and the depolymerization of microtubules caused by salt stress. Moreover, lower Na$^+$ accumulation in shoot and lower H$_2$O$_2$ content are found in *xth30* mutants in response to salt stress. Taken together, these results indicate that XTH30 modulates XyG side chains, altered abundance of XLFG, cellulose synthesis, and cortical microtubule stability, and negatively affecting salt tolerance.**

**Keywords:** Arabidopsis, cellulose, microtubule, salt stress, XLFG, XTH30, xyloglucan.

## Introduction

Salt stress severely reduces plant growth and limits agricultural productivity (Zhu, 2002, 2016). Plants have evolved various strategies to sense and achieve protection against salt stress (Shi *et al.*, 2000; Munns and Tester, 2008). They sense and transmit the stress signal from cell surface to nucleus, then regulate downstream genes to adaptively respond to salt stress (Julkowska and Testerink, 2015; Zhu, 2016).

The plant cell wall is a structural layer outside the cell membrane that provides the cell with both structural support and protection. One of the important plant adaptations to salt stress

is differential regulation of growth, accompanying dynamic changes of the plant cell wall (Tenhaken, 2014; Cosgrove, 2015; Wang *et al.*, 2016). The plant cell wall has a dynamic architecture with cellulose microfibrils embedded in an amorphous matrix of pectin and hemicellulose polysaccharides as well as structural proteins, and in some cells also lignin (Mutwil *et al.*, 2008; Scheller and Ulvskov, 2010). Several genes that are involved in cellulose synthesis, *CesA1*, *CesA6*, and *CesA8*, have been implicated in salt tolerance (Chen *et al.*, 2005; Zhang *et al.*, 2016a). Knocking out either *CesA6* or *CesA1* confers salt stress sensitivity (Zhang *et al.*, 2016a). Companion of cellulose synthase proteins (CC1 and CC2) interact with CesAs and microtubules, and mutations of *CC1* and *CC2* led to salt-sensitive phenotypes by altering microtubule and cellulose synthase complex (CSC) behavior (Endler *et al.*, 2015).

Xyloglucan (XyG) is an important hemicellulose polymer of the primary cell wall in dicotyledons and non–commelinid monocotyledons. XyG plays a vital role in loosening or stiffening the cell wall by binding to cellulose microfibrils with hydrogen bonds during cell elongation (Hayashi and Kaida, 2011; Park and Cosgrove, 2015; Pauly and Keegstra, 2016). XyG has a common backbone of (1–4)-linked β-D-glucopyranosyl residues (β-D-Glu*p*), which can be connected with α-D-xylopyranosyl (α-D-Xyl*p*) residues at O-6 (Cosgrove, 2005). A standard nomenclature using a single letter is used to represent XyG connections. G represents unconnected β-D-Glu*p* residue, while X, L, and F indicate Glc residues connected with α-D-Xyl*p*, β-D-Gal*p*-(1–2)-α-D-Xyl*p*, or α-L-Fuc*p*-(1–2)-β-D-Gal*p*-(1–2)-α-D-Xyl*p* side chains, respectively (Fry *et al.*, 1993). XyG chains can be cleaved or rejoined by xyloglucan endotransglucosylase–hydrolase (XTH) (Nishitani and Tominaga, 1992). Many members of the XTH family in plants have been identified including 33 members in Arabidopsis (Yokoyama and Nishitani, 2001), 29 in rice (Yokoyama *et al.*, 2004), and 22 in barley (Strohmeier *et al.*, 2004). It has been shown that XTHs play a vital role in plant development. During cell wall expansion, *AtXTH27* is highly expressed and can modulate the generation of tracheary elements in Arabidopsis rosette leaves (Matsui *et al.*, 2005). AtXTH21 plays a vital role in the growth of the primary roots by affecting cellulose deposition (Liu *et al.*, 2007). AtXTH28 is involved in automatic self-pollination (Kurasawa *et al.*, 2009). In addition to regulating developmental growth, XTHs are also involved in the response of plants to abiotic stress. Loss–of–function mutation in *AtXTH15* and *AtXTH31* enhances aluminum tolerance (Zhu *et al.*, 2012; Shi *et al.*, 2015). Constitutive expression of a *Capsicum annuum* XTH, *CaXTH3*, in Arabidopsis or tomato improved salt and drought tolerance (Cho *et al.*, 2006; Choi *et al.*, 2011). Overexpression of *Populus euphratica* XTH, *PeXTH*, in tobacco enhanced salt tolerance by the development of leaf succulence (Han *et al.*, 2013). However, the function of XTHs in salt stress and the mechanisms by which XTHs respond to salt stress are still unclear.

In this study, Arabidopsis xyloglucan endotransglucosylase-hydrolase30 (XTH30) was identified as responding to salt stress. *XTH30* loss–of–function mutations led to salt tolerance and gain–of–function resulted in salt sensitivity. Moreover, XTH30 modulated XyG structure, cellulose content and depolymerization of microtubules in response to salt stress.

## Materials and methods

### Plant materials and growth conditions

Arabidopsis (L.) Heynh. ecotype Columbia (Col-0), *xth30-1* (CS16544) and *xth30-2* (CS16543) mutant were obtained from the Arabidopsis Biological Resource Center (ABRC). Homozygous *xth30* mutants were identified by T-DNA insertion-based PCR using the specific primers listed in Supplementary Table S1 at *JXB* online. The *xth30* mutants (*xth30-1* and *xth30-2*) were crossed with transgenic Arabidopsis expressing green fluorescent protein (GFP)-tagged α-tubulin 6 isoform (*35S:GFP-TUA6*) for the observation of cortical microtubules.

Seeds were sterilized and sown on a solid medium containing half-strength Murashige and Skoog salts including vitamins and 1% (w/v) sucrose at 4 °C for 2 d and then grown in a growth chamber (22 °C, 100–200 µmol m$^{-2}$ s$^{-1}$, 14 h light/10 h dark, 60% humidity).

### Phenotypic analysis

For a salt sensitivity assay on plates, 5-day-old seedlings grown on 1/2 MS medium were transferred onto 1/2 MS medium with mannitol or salt added as described and allowed to grow for an additional 7 d. Seedlings were photographed and freshly weighed.

For the hydroponic salt sensitivity assay, 3-week-old seedlings were treated with nutrient solution as described in Fang *et al.* (2016) containing 125 mM NaCl and allowed to grow for an additional 9 d. After recovery with normal nutrient solution for 3 d, the seedlings were photographed and the survival rate was calculated.

For a heavy metal stress ($Zn^{2+}$ and $Cd^{2+}$) tolerance test, 5-day-old seedlings grown on 1/2 MS medium were transferred onto 1/2 MS medium with 50 µM $CdCl_2$ and 500 µM $ZnSO_4$, then allowed to grow for an additional 7 d. For ABA treatments, 5-day-old seedlings grown on 1/2 MS medium were transferred onto 1/2 MS medium with 20 µM ABA, then allowed to grow for an additional 7 d. Seedlings were photographed after various treatments.

### Determination of Na$^+$ content

Shoots and roots of Arabidopsis seedlings were harvested separately, and Na$^+$ content was measured according to the methods described by Wang *et al.* (2015). Briefly, dry samples were digested in 1 ml of nitric acid at 90 °C for 12 h, diluted to 5 ml with distilled water, and then analysed using an inductively coupled plasma-optical emission spectrometry instrument (Pekin Elmer, USA).

### Hypocotyl length measurements

For isoxaben and oryzalin treatments, seeds were sown on 1/2 MS medium plates supplemented with or without 2 nM isoxaben or 400 nM oryzalin (Sigma-Aldrich, USA) and grown for 6 d in the dark. For salt treatments, 2-day-old etiolated seedlings were transferred to 1/2 MS plates containing 100 mM NaCl for another 5 d in the dark. The hypocotyl lengths were quantified using the ImageJ program.

### Vector construction and generation of transgenic plants

The full-length *XTH30* with no stop codon was amplified by PCR using the specific primers (Supplementary Table S1) and cloned into the pEarleyGate 101 vector using the BP and LR clonase reaction (Invitrogen, USA). The recombinant plasmid was sequenced and introduced to Col-0 and *xth30-1* mutant by *Agrobacterium tumefaciens* strain GV3101-mediated transformation. Positive transformants were selected on 1/2 MS medium containing 25 µg ml$^{-1}$ DL-phosphinothricin (Sigma-Aldrich). The resistant T2 seedlings with 3:1 segregation of resistance were transferred to soil to obtain homozygous T3 seeds from individual lines.

### Seed germination assays

More than 100 seeds were sown on 1/2 MS medium containing 1% sucrose with or without 125 mM NaCl. The plates were stratified at 4 °C for 48 h, and placed at 22 °C under light conditions. Radicle emergence of >1 mm was counted every day for germination analysis.

## Real-time PCR analysis

Total RNA was extracted from seedlings or etiolated hypocotyls using the RNeasy Plant Mini Kit (Qiagen, USA). RNA was first treated with DNase I (Sigma-Aldrich), and first-stand cDNA synthesis was performed using the iScript cDNA Synthesis Kit (Bio-Rad, USA) according to the manufacturer's protocol. Real-time RT-PCR was performed using SYBR Select Master Mix (Applied Biosystems, USA) on diluted (5 times) cDNA using the StepOne Plus Real-Time PCR System (Applied Biosystem 7500). The specific primers are listed in Supplementary Table S1. The relative expression levels were determined using the $2^{-\Delta\Delta CT}$ method as described in (Yan *et al.*, 2015).

## Determination of $H_2O_2$ level

For quantification of $H_2O_2$, 3-week-old hydroponically grown seedlings were treated with nutrient solution containing 125 mM NaCl for 6 d, and shoots were harvested. $H_2O_2$ content was determined by a horseradish peroxidase-based spectrophotometric assay following the protocol described by Pierce™ Quantitative Peroxide Assay Kit (Aqueous) (Thermo Fisher Scientific, USA).

## Antioxidant enzyme assay

Three-week-old hydroponically grown seedlings were treated with nutrient solution containing 125 mM NaCl for 6 d, and shoots were harvested. The samples were homogenized in 1 ml of 50 mM potassium phosphate buffer (pH 7.0) containing 1 mM EDTA and 1% polyvinyl-pyrrolidone, with the addition of 1 mM sodium ascorbate. The homogenate was centrifuged at 12 000 *g* for 30 min at 4 °C, and then the supernatant was used for measuring the activities of antioxidant enzymes as previously described (Huang *et al.*, 2013).

## Subcellular localization of XTH30

The *XTH30* coding sequence was fused to yellow fluorescent protein (YFP) at the N-terminus driven by *35S* promoter (*XTH30-YFP*). Four-week-old *Nicotiana benthamiana* leaves were co-infiltrated with *Agrobacterium tumefaciens* strain GV3101 carrying the *35S::XTH30-YFP* fusion construct and the *AtPIP2A-mCherry* marker (pm-rk) as described by Nelson *et al.* (2007). The plasmolysed tobacco cells were observed by treatment with 300 mM mannitol for 10 min. The microscopy was performed using a Zeiss LSM710 device as previously described (Zhu *et al.*, 2016).

## Plasma membrane isolation

The leaves of *OX#1* seedlings were harvested and homogenized in a solution (50 mM Tris–HCl, pH 7.5, 1 mM EDTA, 10 mM KCl, 0.5 mM phenylmethylsulfonyl fluoride and 2 mM dithiothreitol) and centrifuged at 6000 *g* for 10 min at 4 °C. The supernatant was centrifuged at 100 000 *g* for 45 min, the pellet was used as total microsomal membrane proteins, and the supernatant was regarded as cytosolic proteins.

## XTH30 promoter::GUS construct and GUS activity

A 2000 bp promoter region of *XTH30* was amplified by PCR using the specific primers listed in Supplementary Table S1. The PCR product was cloned into the pGWB3 vector using the BP and LR clonase reaction (Invitrogen). The recombinant plasmid was sequenced and introduced into Col-0 by *Agrobacterium tumefaciens* strain GV3101-mediated transformation. Positive transformants were selected on 1/2 MS medium containing 50 μg ml$^{-1}$ hygromycin (Omega Scientific, USA). Various tissues were submerged in X-Gluc buffer (50 mM sodium phosphate buffer, pH 7.0, 1 mM EDTA, 0.5 mg ml$^{-1}$ 5-bromo-4-chloro-3-indolyl β-D-GlcUA [X-Gluc] (Sigma-Aldrich), 0.4% Triton X-100, 5 mM potassium ferricyanide, and 5 mM potassium ferrocyanide) and incubated at 37 °C overnight in the dark, followed by washing with 70% ethanol to remove chlorophyll as described in Lee *et al.* (2015).

## Cell wall preparation

For quantification of the crystalline cellulose fraction and XyG contents, 2-day-old etiolated seedlings were transferred to 1/2 MS plates containing 100 mM NaCl for another 5 d. The fresh samples were harvested into 96% ethanol and incubated for 30 min at 100 °C to inactivate cell wall-degrading enzymes. The tissue was homogenized using a Retsch MM200 mixer mill and centrifuged. The pellet was washed with 100% ethanol and twice with a mixture of chloroform and methanol (2:1), followed by four successive washes with 100% ethanol and acetone. The pellet was air-dried overnight and is referred to as alcohol-insoluble residue (AIR).

## Crystalline cellulose content

The crystalline cellulose content was determined as described (Fang *et al.*, 2016). In brief, the pellet was air-dried overnight. The starch in the samples was degraded with α-amylase, amyloglucosidase, and pullulanase (Megazyme, Brae, Ireland). Destarched AIR (2 mg) was hydrolysed in 2 M trifluoroacetic acid (TFA) at 121 °C for 1 h. Then the TFA-insoluble material was washed with water and further hydrolysed with 72% (v/v) sulfuric acid containing 10 mg *myo*-inositol for 1 h at room temperature. The sulfuric acid was then diluted to 1 M with water and the samples further incubated at 100 °C for 3 h; they were neutralized with barium carbonate (BaCO$_3$) to provide the crystalline cellulose fraction and analysed by high performance anion exchange chromatography (HPAEC) on an ICS-5000 instrument (Thermo Fisher Scientific) equipped with a CarboPac PA20 (3 mm×150 mm, Thermo Fisher Scientific) analytical anion exchange column, PA20 guard column (3 mm×30 mm), borate trap, and a 500 pulsed amperometric detector. The *myo*-inositol was used as an internal standard.

## MALDI-TOF mass spectrometry analysis of XyG oligosaccharides

To analyse the XyG, we used the rapid phenotyping method using enzymatic oligosaccharide fingerprinting as used in Lerouxel *et al.* (2002). Two-day-old seedlings grown in the dark on 1/2 MS medium were transferred to 1/2 MS medium with or without 100 mM NaCl, and then grown for 5 d. The hypocotyl was stored in 100% ethanol. After ethanol removal and rehydration, XyG oligosaccharides were generated by treating with 1 unit of xyloglucanase (Megazyme) or endoglucanase (Megazyme) in 50 mM sodium acetate buffer (pH 5.0) overnight at 37 °C. Matrix-assisted laser-desorption ionization time of flight mass spectrometry of the XyG oligosaccharides was recorded with an Applied Biosystems 4800 MALDI/TOF mass spectrometer using super-DHB (Sigma-Aldrich) as matrix.

## Xyloglucan content quantified by iodine staining

XyG content was measured using iodine staining as in Kooiman (1960) and Vuttipongchaikij *et al.* (2012) with minor modifications. In brief, 2-day-old etiolated seedlings were transferred to 1/2 MS plates containing 100 mM NaCl for another 5 d in dark. The AIR was extracted from hypocotyl. Hemicellulose material was isolated from de-starched AIR by incubating with 4 M KOH containing 1% sodium borohydride overnight. The supernatant were neutralized with glacial acetic acid on ice and dialysed in dialysis tubing (Spectra/Por6 3000 MWCO; Spectrum, USA) against water. The dialysed material was freeze-dried and dissolved in water. A 200 μl portion of each sample was mixed with 112 μl of 20% Na$_2$SO$_4$ and 28 μl of Lugol's solution (Sigma-Aldrich). After incubation for 1 h at room temperature, the absorbance was determined at 640 nm. Tamarind (*Tamarindus indica*) xyloglucan (Megazyme) was used as a standard.

## Microtubule observation

Both wild type and *xth30* mutant seeds expressing *35S:GFP-TUA6* were grown on 1/2 MS medium for 3 d and then transferred to 1/2 MS

medium with 100 mM NaCl or 10 μM oryzalin. After the indicated treatments, the cortical microtubules in etiolated hypocotyls were observed under a confocal microscope (Zeiss LSM710) with an excitation at 488 nm and emission at 533 nm.

## Results

### The expression of XTH30 *is strongly induced by salt stress*

*XTH30* expression was examined in order to investigate whether it responds to salt stress. As shown in Fig. 1A, the expression of *XTH30* was strongly induced at 6 h, maximal at 12 h, and then decreased at 24 h after 150 mM NaCl treatment.

The *XTH30* expression in various tissues was also investigated. The results showed that *XTH30* accumulated at high levels in root, stem, and flower but at low levels in rosette leaves and cauline leaves (Fig. 1B). Besides that, the 2.0 kb promoter region of *XTH30* was fused to a β–glucuronidase (GUS) reporter gene. GUS activity was strongly detected in root and etiolated hypocotyl but weakly observed in leaves, which was further increased by NaCl treatment (Fig. 1C). These results are consistent with the qRT-PCR results.

### XTH30 negatively affects salt stress tolerance

To determine the role of XTH30 in plants under salt stress, two independent mutants of *XTH30* with T-DNA insertion (*xth30-1*
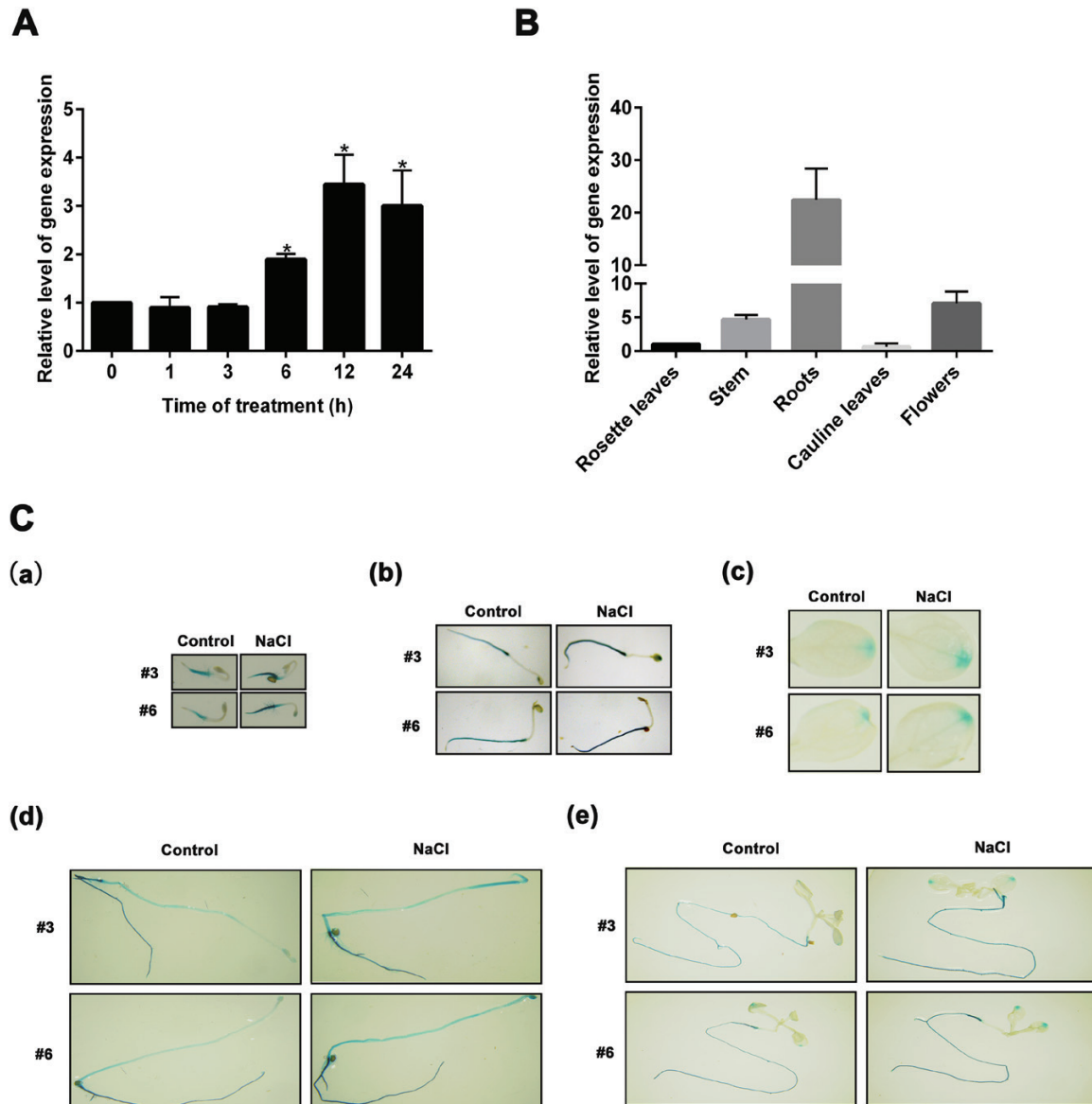


**Fig. 1.** Expression pattern of *XTH30* in Arabidopsis. (A) Expression of *XTH30* in Arabidopsis seedlings in response to salt stress. Fourteen-day-old seedlings were treated with 150 mM NaCl for different time as indicated. (B) Expression of *XTH30* in rosette leaves, stem, roots, cauline leaves, and flowers. (C) *XTH30 promoter::GUS* expression patterns under salt stress in various developmental stages. *XTH30 promoter::GUS* expression of two lines (no. 3 and no. 6) in 3-day-old seedling (a), 5-day-old seedling (b), leaves (c), 7-day-old etiolated hypocotyl (d), and roots (e) exposed to salt stress. Seedlings in (a, b) were treated with 150 mM NaCl for 1 h. Seedlings in (c–e) were treated with 150 mM NaCl for 12 h. Error bars represent SD (*n*=3) in (A, B). *ACTIN 2* acts as a reference standard. The asterisk in (A) indicates a significant difference compared with the control using unpaired Student's *t*-test (*$P<0.05$). Experiment in (B) was performed at least three times with similar results. (This figure is available in color at *JXB* online.)

and *xth30-2*) were used to perform salt sensitivity assays. The T-DNA insertion in both *xth30-1* and *xth30-2* is located in the third intron of *XTH30* genome and was confirmed by PCR using specific primers as indicated in Supplementary Fig. S1. When 5-day-old seedlings of the wild type and *xth30* mutants were transferred to 1/2 MS medium with 125 mM NaCl, *xth30* mutants showed more tolerance than the wild type (Fig. 2A). To completely investigate the function of XTH30, we expressed *XTH30* in the *xth30-1* knock-out background (*com#1* and *com#3*) as well as in Col-0 (*OX#1* and *OX#5*) (Supplementary Figs S2, S3). As shown in Fig. 2C, E, *com#1* and *com#3* were more sensitive to salt stress than *xth30-1* and performed similarly to the wild type, and both *OX#1* and *OX#5* lines showed hypersensitivity to salt stress compared with the wild type.

Hydroponically grown seedlings of *xth30-1* and *xth30-2* were also used to confirm the role of XTH30. The *xth30* mutants wilted less and showed a much higher survival rate than the wild type under 125 mM NaCl treatment (Supplementary Fig. S4). These results indicate that XTH30 negatively affects salt stress tolerance. No growth phenotype difference was observed between *xth30* mutants and the wild type under heavy metal stresses ($CdCl_2$ and $ZnSO_4$) or the plant hormone abscisic acid (ABA) treatment (Supplementary Fig. S5).

To investigate the role of XTH30 in more detail, the seedling fresh weight of *xth30*, *com*, *OX*, and wild type was measured. As shown in Fig. 2B, D, F, compared with wild type, *xth30* showed a higher seedling fresh weight, *com* showed similar performance, and *OX* showed a lower fresh weight. Salt stress results
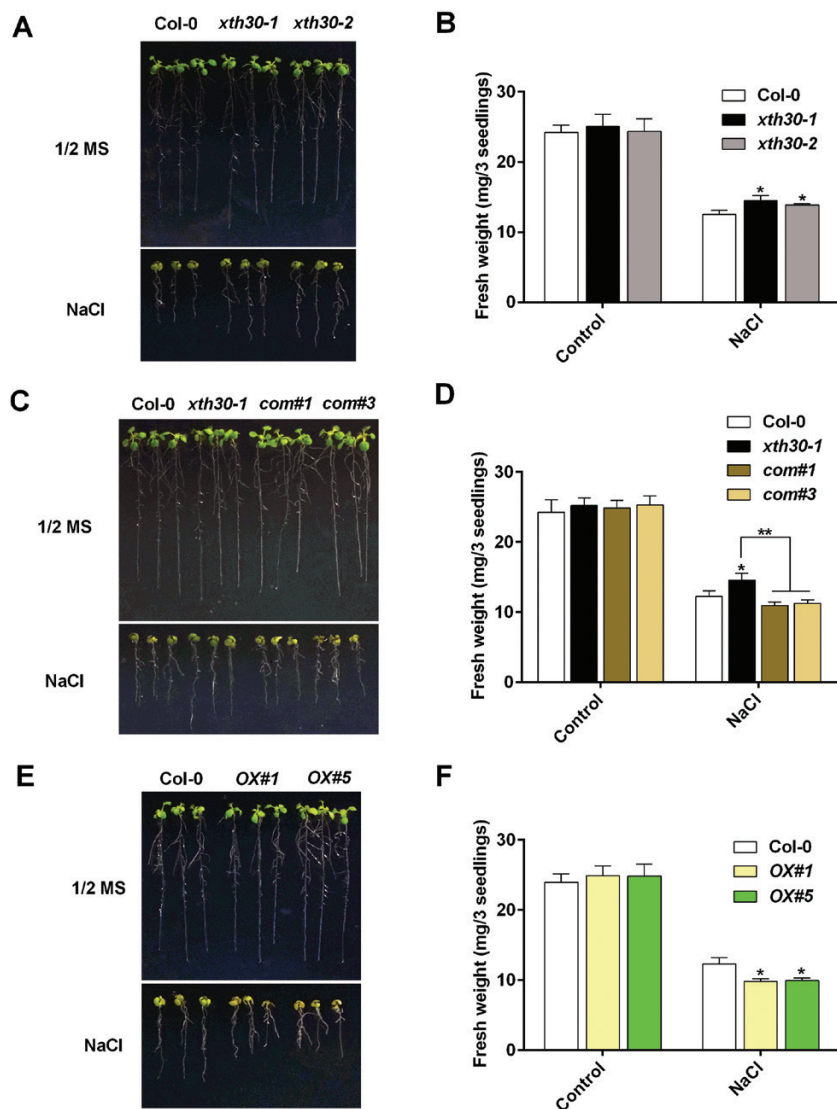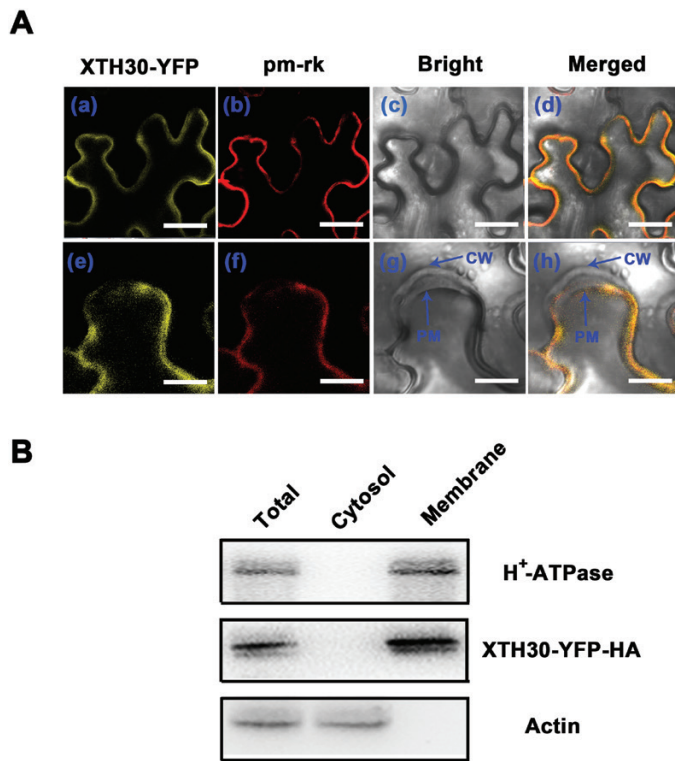


**Fig. 2.** *XTH30* negatively affects salt stress tolerance. (A) Analysis of salt sensitivity in *xth30* mutants. Five-day-old seedlings of *xth30-1*, *xth30-2*, and Col-0 grown on 1/2 MS medium were transferred to 1/2 MS medium with or without 125 mM NaCl. Photographs were taken after 7 d of treatment. (B) Fresh weight of seedlings tested in (A). (C) Analysis of salt sensitivity in complementation of *XTH30* in *xth30-1* (*com#1* and *com#3*). Five-day-old seedlings of *xth30-1*, complementation of *XTH30* in *xth30-1* (*com#1* and *com#3*), and Col-0 grown on 1/2 MS medium were transferred to 1/2 MS medium with or without 125 mM NaCl. Photographs were taken after 7 d of treatment. (D) Fresh weight of seedlings tested in (C). (E) Analysis of salt sensitivity in *XTH30* overexpressors (*OX#1* and *OX#5*). Five-day-old seedlings of *XTH30* overexpressors (*OX#1* and *OX#5*) and Col-0 grown on 1/2 MS medium were transferred to 1/2 MS medium with or without 125 mM NaCl. Photographs were taken after 7 d of treatment. (F) Fresh weight of seedlings tested in (E). Data in (B, D, F) are means ±SD (*n*=3). The asterisks indicate a significant difference between various genotypes and wild type using unpaired Student's *t*-test (*$P<0.05$, **$P<0.01$). (This figure is available in color at *JXB* online.)

in both osmotic and ionic stress in plant (Munns and Tester, 2008). Next we determined whether salt tolerance of *xth30* mutants is a specific response to the sodium ions. As shown



**Fig. 3.** Subcellular localization of XTH30. (Aa–d) *Nicotiana benthamiana* leaf cells co-expressing XTH30–YFP fusion protein (a), plasma membrane marker (pm-rk) (b), bright-field image (c), and with a merged image (d) in a non-plasmolysed tobacco cell. (Ae–h) *Nicotiana benthamiana* leaf cells co-expressing XTH30–YFP fusion protein (e), plasma membrane marker (pm-rk) (f), bright-field image (g), and with a merged image (h) in a plasmolysed tobacco cell by treatment with 300 mM mannitol for 10 min. Scale bars indicate 20 μm in (a–d), and 10 μm in (e–h). CW, cell wall; PM, plasma membrane. (B) Immunoblotting assay showing XTH30 localization. Two-week-old seedlings of *OX#1*, which expressed XTH30–YFP–HA fusion protein, were harvested. Plasma membrane and cytosol fractions were isolated, and the YFP–HA-tagged XTH30 was detected by HA antibody. Actin acts as a cytosol protein marker; $H^+$-ATPase acts as a membrane protein marker. Similar results in (A, B) were from repeats of at least three times. (This figure is available in color at *JXB* online.)

in Supplementary Fig. S6, seedlings of *xth30-1* and *xth30-2* respond to $Na^+$ and $Li^+$, but not $K^+$, $Cl^-$, and osmotic stress, which was a similar behavior to *sos* mutants (Shi *et al.*, 2000; Zhu, 2002). No significant difference was observed between the wild type and *xth30* mutants in seed germination under salt stress (Supplementary Fig. S7) or in growth under normal conditions (Supplementary Fig. S8).

One of the most damaging effects of high salinity is the accumulation of salt in plants, and so $Na^+$ content was investigated. The results showed that under 125 mM NaCl treatment, $Na^+$ accumulated more in the wild type than in *xth30* mutants in shoots, and there was no difference in $Na^+$ accumulation between the wild type and *xth30* mutants in roots (Supplementary Fig. S9). Salt stress leads to the overproduction of reactive oxygen species (ROS), which are highly reactive and toxic (Ma *et al.*, 2012; Ben Rejeb *et al.*, 2015). To understand the role of XTH30 in salt stress, we investigated $H_2O_2$ production in *xth30* mutants and wild type seedlings under salt stress. When seedlings were grown on the 1/2 MS medium, the wild type and *xth30* mutants showed a similar basal level of $H_2O_2$ (Supplementary Fig. S10). $H_2O_2$ levels increased both in the wild type and *xth30* mutants after 125 mM NaCl treatment, and a relatively much smaller $H_2O_2$ increase was observed in *xth30* mutants (Supplementary Fig. S10). We also measured the activities of antioxidant enzymes (catalase (CAT) and peroxidase (POD)) that are responsible for removing $H_2O_2$. As shown in Supplementary Fig. S11, the activities of CAT and POD increased both in the wild type and *xth30* mutants exposed to NaCl treatment, and a greater increase was observed in *xth30* mutants than in the wild type.

## XTH30 is located in the plasma membrane

XTHs were shown to be localized to endoplasmic reticulum, cell wall, or plasma membrane (Genovesi *et al.*, 2008; Zhu *et al.*, 2012; Han *et al.*, 2013). To understand the functions of XTH30, its subcellular localization was investigated. As shown in Fig. 3, XTH30–YFP protein was observed around the cell periphery consistent with plasma membrane-localized marker (pm–rk) (Nelson *et al.*, 2007), suggesting that XTH30 was localized in plasma membrane (Fig. 3Aa–d). To clearly determine the plasma
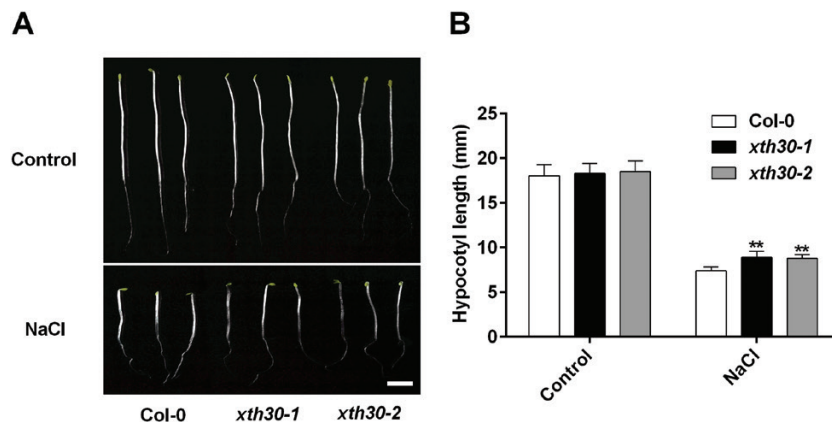


**Fig. 4.** XTH30 affects etiolated hypocotyl growth in response to salt stress. (A) Seedlings germinated and grown for 2 d on 1/2 MS plates and transferred to 1/2 MS plates supplemented with or without 100 mM NaCl and grown for an additional 5 d in the dark. (B) Quantification of hypocotyl elongation of seedlings in (A). Error bars represent SD; *n*>15 seedlings per biological replicate. Similar results were observed in three independent experiments. The asterisk indicates a significant difference between *xth30* mutants and wild type using unpaired Student's *t*-test (**$P<0.01$). Scale bar indicates 3 mm.

membrane location of XTH30, plasmolysis was performed. The results showed that XTH30 was localized in the plasma membrane but not in the cell wall (Fig. 3Ae–f). In order to further confirm the localization of XTH30, the plasma membrane and cytoplasmic fractions were isolated from *XTH30* overexpressor (*OX#1*). The isolated plasma membrane fractions were confirmed by the marker, H⁺–ATPase. Consistent with the results of *XTH30* expression in tobacco cell, XTH30–YFP–HA was only detected in plasma membrane (Fig. 3B).

### XTH30 affects the xyloglucan oligosaccharide composition during salt stress

To further understand the role of XTH30 in plants under salt stress, etiolated hypocotyl of Arabidopsis seedling was used. It is widely used to study plant primary cell wall because no cell division occurs in the dark and growth is due to cell elongation only (Refrégier *et al.*, 2004; Endler *et al.*, 2015; Xiao *et al.*, 2016). As shown in Fig. 4, the etiolated hypocotyl in *xth30* mutants was longer than that in the wild type under salt stress. This indicated that XTH30 negatively modulated the salt tolerance during cell elongation in etiolated Arabidopsis seedlings.

XTHs can cleave or rejoin XyG chains, resulting in the modification of content or structure of XyG (Nishitani and Tominaga, 1992), and XyG is shown to cross-link adjacent cellulose microfibrils and modulate cell wall extensibility in response to environmental variation (Hayashi *et al.*, 2010), which prompted us to investigate the XyG content. Iodine staining (Kooiman, 1960; Gille *et al.*, 2011; Vuttipongchaikij *et al.*, 2012) was used to measure the amount of XyG in de-starched alkaline extracts from *xth30* mutants and wild-type etiolated hypocotyls. Unexpectedly, the extractable XyG content in *xth30* mutants was similar to that in the wild type after 100 mM NaCl treatment (Fig. 5A). These results suggest that XTH30 does not affect XyG content.

Next we analysed the XyG structure from etiolated hypocotyls. Xyloglucan was treated with xyloglucanase, which attacks unconnected Glc residues and produces an oligosaccharide mixture that includes GXXG, XXXG, XXLG, XXFG, XXFG+Ac, XLFG, and XLFG+Ac (Gille *et al.*, 2011). As shown in Fig. 5B, salt stress decreased the relative level of XXFG and XXFG+Ac, but increased the level of XXXG, XLFG, and XLFG+Ac in the wild type. More importantly, the increase of XLFG caused by salt stress in the wild type was partly blocked in *xth30* mutants (Fig. 5B). To confirm the effect of XTH30 on XLFG content, another enzyme, endoglucanase (Sechet *et al.*, 2016), was used. As expected, similar changes were also observed by digesting with endoglucanase (Fig. 5C). These results indicate that XTH30 plays an important role in the accumulation of the largely connected XyG oligosaccharides XLFG in response to salt stress.
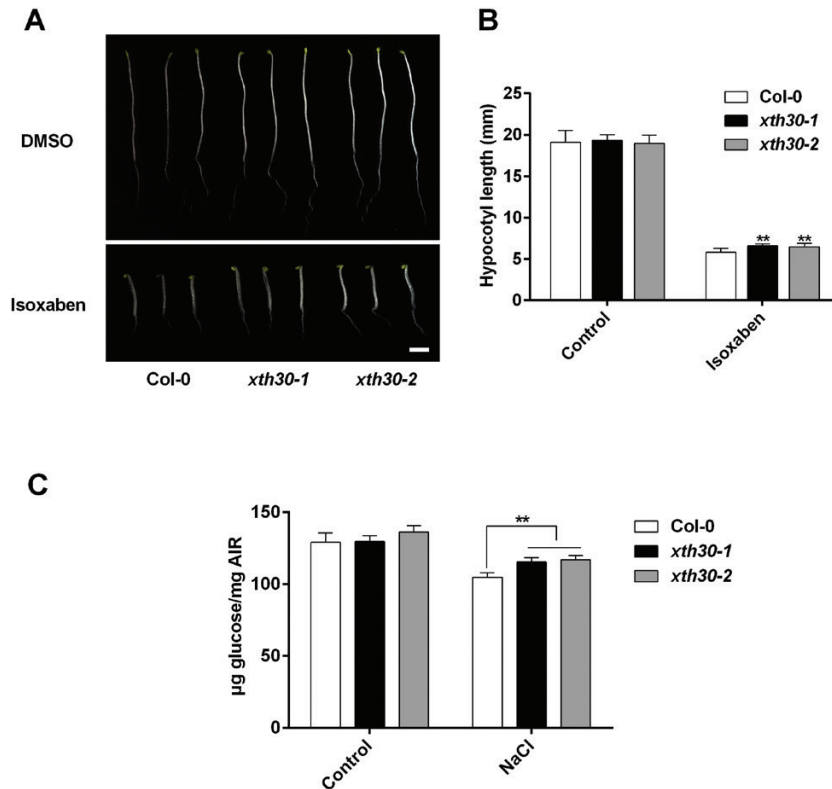
### XTH30 affects cellulose synthesis under salt stress

XyG affects cellulose biosynthesis (Xiao *et al.*, 2016). To explore whether cellulose synthesis is also affected in *xth30* mutants, we first used the cellulose synthesis inhibitor
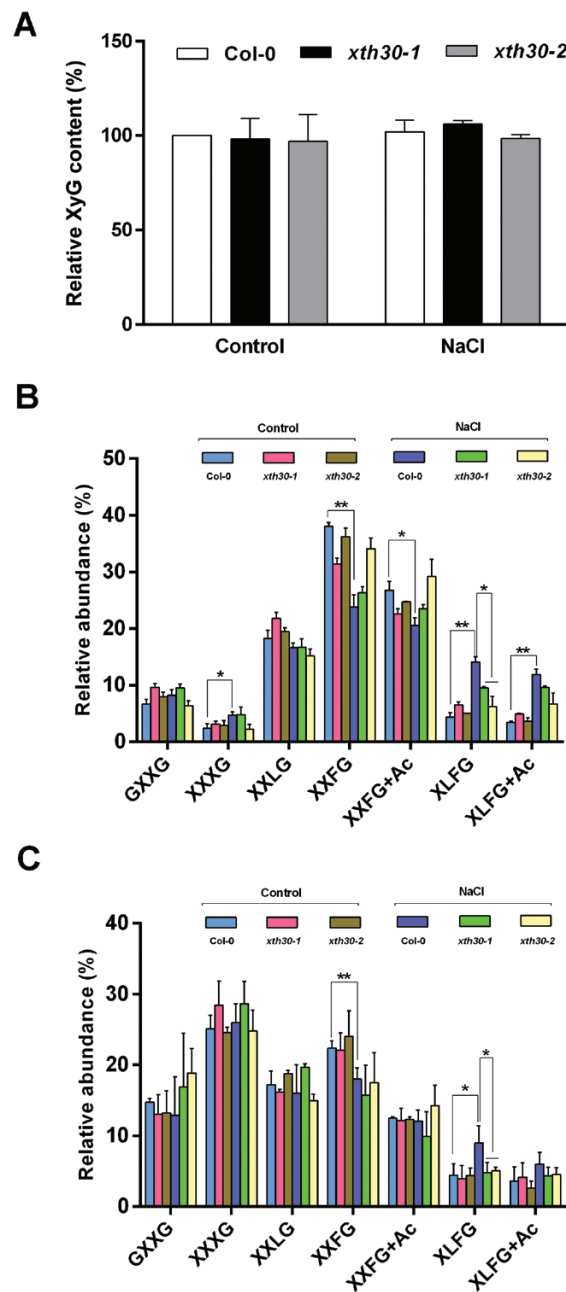


**Fig. 5.** XTH30 affects XyG oligosaccharides in response to salt stress. (A) Extractable XyG content of hypocotyl quantified by iodine staining. Two-day-old etiolated seedlings were transferred to 1/2 MS plates containing 100 mM NaCl for another 5 d in the dark. The AIR was extracted from hypocotyl. Data are presented as percentage of the content of wild type (Col-0). Error bars represent SD (*n*=3). (B) XyG oligosaccharides generated from hypocotyl with xyloglucanase. (C) XyG oligosaccharides generated from hypocotyl with endoglucanase. Relative abundance of major subunits in (B, C) is shown as means of three biological replicates with SD. The asterisks indicate a significant difference between *xth30* mutants and the wild type using unpaired Student's *t*-test (*$P<0.05$, **$P<0.01$). (This figure is available in color at *JXB* online.)

isoxaben (Lei *et al.*, 2014; Zhang *et al.*, 2016b). We grew the *xth30* mutants and the wild type on 1/2 MS medium supplemented with isoxaben, and found that the *xth30* mutants were less sensitive to growth inhibition by isoxaben than was the wild type (Fig. 6A, B). These results suggest that XTH30 might be involved in cellulose synthesis. Next, we

**Fig. 6.** XTH30 affects cellulose synthesis under salt stress. (A) Seedlings germinated and grown for 6 d on 1/2 MS supplemented with or without 2 nM isoxaben in dark. Scale bar indicates 3 mm. (B) Quantification of hypocotyl elongation of seedlings in (A). Error bars represent SD, *n*>15 seedlings per biological replicate. Similar results were observed in three independent experiments. (C) Crystalline cellulose content of hypocotyl from *xth30* mutants and wild type in response to salt stress. Error bars represent SD (*n*=3). The asterisks in (B, C) indicate a significant difference between *xth30* mutants and wild type using unpaired Student's *t*-test (\*\**P*<0.01).

estimated the crystalline cellulose content. Salt stress significantly decreased the crystalline cellulose content in the wild type (Fig. 6C), which is consistent with a previous report (Endler *et al.*, 2015). The cellulose synthesis genes (*CesA1*, *CesA3*, *CesA6*) were then analysed by qRT-PCR. The results showed that salt stress increased *CesA3* and *CesA6* expression in both the wild type and *xth30* mutants, which was not affected by the loss of *XTH30* (Supplementary Fig. S12). However, the decrease of crystalline cellulose content resulting from salt stress was much smaller in *xth30* mutants (Fig. 6C). These suggest that XTH30 affects cellulose synthesis under salt stress.

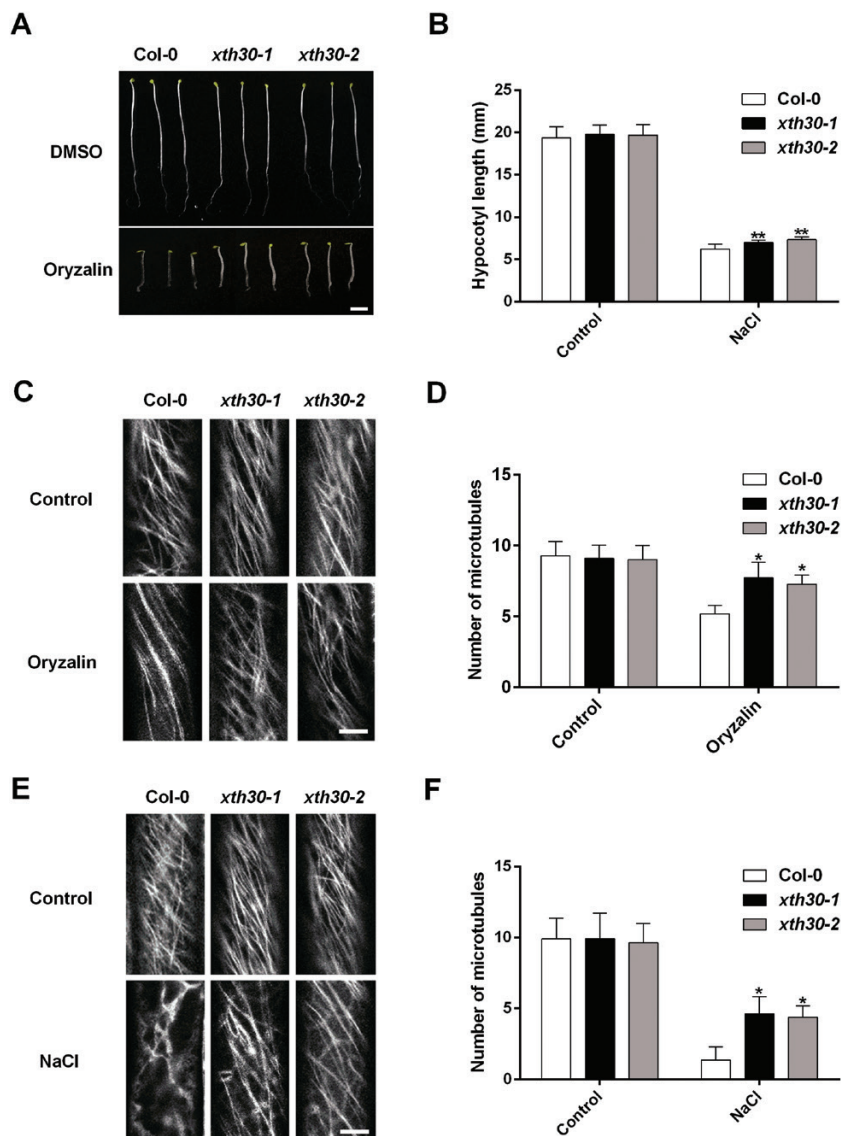### XTH30 aggravates depolymerization of cortical microtubules under salt stress

Cellulose microfibrils are typically transversely organized and can align with cortical microtubules that are tethered to the plasma membrane (Labavitch and Ray *et al.*, 1974; Hayashi *et al.*, 1984; Park and Cosgrove, 2015). Next, we analysed the effects of XTH30 on cortical microtubules. Oryzalin, a microtubule depolymerizing agent, was used (Endler *et al.*, 2015), and the etiolated hypocotyl growth of *xth30* mutants was less inhibited by oryzalin (Fig. 7A, B). Then, we generated transgenic lines that expressed the microtubules marker GFP–TUA6 (Arabidopsis α-tubulin 6 isoform fused to GFP) driven by the *35S* promoter in the *xth30* mutants and Col-0 to observe the

cortical microtubule (Zhang *et al.*, 2012). Treatment with 10 μM oryzalin triggered depolymerization of microtubules in the wild type and *xth30* mutants, and the wild type showed more depolymerization than *xth30* mutants (Fig. 7C, D). To further investigate the effect of XTH30 on cortical microtubules under salt stress, 3-day-old etiolated seedlings were transferred to 1/2 MS medium with or without 100 mM NaCl for 12 h. Under normal conditions, there is no obvious depolymerization of cortical microtubules in both *xth30* mutants and the wild type (Fig. 7E, F). However, in the presence of NaCl, we observed obvious depolymerization of microtubules both in the wild type and *xth30-1* mutants, and the wild type showed a more severe depolymerization compared with *xth30* mutants (Fig. 7E, F). These results indicate that XTH30 aggravates depolymerization of cortical microtubules in response to salt stress.

## Discussion

As a structural layer outside the cell membrane, the plant cell wall not only provides the cell with structural support but also acts as the first line of defense against various stresses. The cell wall is flexible so that it can be rapidly remodeled when subjected to developmental, biotic, or abiotic stimuli. Maintaining the synthesis/deposition of cellulose is vital for the tolerance to salt stress. Several genes involved in cellulose synthesis (such as *CesA1* and *CesA6*) as well as companions of cellulose synthase proteins (CC1 and CC2) have been found to function

**Fig. 7.** Knockout of *XTH30* alleviates depolymerization of cortical microtubules under salt stress. (A) Seedlings germinated and grown for 6 d on 1/2 MS with or without 400 nM oryzalin in dark. (B) Quantification of hypocotyl elongation of seedlings in (A). Error bars represent SD, *n*>15 seedlings per biological replicate. Similar results were observed in three independent experiments. (C) Confocal images of GFP–TUA6 labeled cortical microtubules. Three-day-old etiolated seedlings were exposed to 10 μM oryzalin for 5 min. The epidermal cells in etiolated hypocotyls were observed. (D) Quantification of hypocotyl elongation of seedlings in (C). (E) Confocal images of GFP–TUA6 labeled cortical microtubules. Three-day-old etiolated seedlings were exposed to 100 mM NaCl for 12 h. The epidermal cells in etiolated hypocotyls were observed. (F) Quantification of hypocotyl elongation of seedlings in (E). The number of cortical microtubules in (D, F) was determined by counting the microtubules across a fixed line (~10 μm) vertical to the orientation of the most cortical microtubules of the cell. Data in (D, F) represent the mean ±SD of three independent experiments with a minimum of 10 cells from three seedlings assessed in each experiment. Scale bar in (A) indicates 3 mm, and scale bar in (C, E) indicates 5 μm. The asterisks in (B, D, F) indicate a significant difference between *xth30* mutants and wild type using unpaired Student's *t*-test (*$P<0.05$, **$P<0.01$).

in salt stress responses, and knockout of these genes resulted in salt stress sensitivity (Endler *et al.*, 2015; Zhang *et al.*, 2016*a*). However, the mechanisms of cell wall function in plant response to stresses are largely unknown. In this study, we revealed that an XTH, XTH30, negatively affected salt tolerance.

XTH enzymes play a role in cell wall loosening and therefore can affect cell expansion. Unlike mutants of other members of the XTH family, such as *XTH21*, *XTH27*, *XTH28*, and *XTH31* (Matsui *et al.*, 2005; Liu *et al.*, 2007; Kurasawa *et al.*, 2009; Zhu *et al.*, 2012), *xth30* mutants do not have an obvious growth phenotype (Supplementary Fig. S8). However, *xth30* mutants showed a very different performance from the wild type when subjected to salt stress. We found that XTH30

negatively affected salt tolerance based on the following evidence. First, knock-out mutations in *XTH30* led to a salt-tolerant phenotype during growth of seedlings and etiolated hypocotyls (Figs 2A, B, 4; Supplementary Figs S4, S6). Second, overexpression of *XTH30* enhanced sensitivity to salt stress (Fig. 2E, F). Cho *et al.* (2006) found that *CaXTH3* participated in the protection of Arabidopsis mesophyll cells from salt stress via strengthening the cell wall layers. *PeXTH* positively modulated salt tolerance in tobacco by mainly affecting the development of leaf succulence (Han *et al.*, 2013). XTH30 is another XTH member that is found to respond to salt stress (Cho *et al.*, 2006; Choi *et al.*, 2011; Han *et al.*, 2013). However, these XTH genes (*CaXTH3* and *PeXTH*) act as positive

regulators in response to salt stress. The XTH enzymes encoded by numerous *XTH* genes could cleave or re-ligate the xyloglycan chains in the plant cell wall by its two reverse functions, xyloglucan endotransglucosylase (XET) activity and/or xyloglucan endohydrolase (XEH) (Thompson and Fry, 2001; Nishikubo *et al.*, 2011). This implies that members of the XTH family might have different roles in the same process.

XTH can cleave or rejoin XyG chains and change the XyG size in the primary cell wall (Thompson and Fry, 2001; Nishikubo *et al.*, 2011; Park and Cosgrove, 2015). XyG is the most abundant hemicellulose in the primary cell wall in dicots. XyG often undergoes turnover by wall-localized enzymes during cell elongation (Hayashi *et al.*, 1984). In this study, we observed that *XTH30* did not affect the extractable XyG content and the abundance of XyG oligosaccharides, i.e. XXXG, XXLG, and XXFG, under salt stress (Fig. 5). However, we found that loss-of-function of *XTH30* obviously suppressed the strong increases in the abundance of XyG side chain, XLFG, in the wild type under salt stress (Fig. 5B, C). Loss of *MUR3* resulted in shorter etiolated hypocotyl phenotype due to the altering of galactose depleted–xyloglucan (Tamura *et al.*, 2005; Kong *et al.*, 2015). The altered side chain of XyG in the cell wall is more deleterious to cellular processes than the complete absence of xyloglucan (Xu *et al.*, 2017). The salt-tolerant phenotype of *xth30* mutants might be due to the relatively stable XyG side chain. This is also similar to the report that the *mur3-1* mutant with altered XyG side chain is hypersensitive to salt stress (Li *et al.*, 2013).

XyG binds tightly to cellulose within the primary cell wall, coating most available cellulose surfaces during their synthesis and tethering adjacent microfibrils to major load-bearing networks in the growing cell wall (Labavitch and Ray *et al.*, 1974; Hayashi *et al.*, 1984; Park and Cosgrove, 2015). Overexpression of *AtXTH21* in Arabidopsis enhanced the deposition of cellulose (Liu *et al.*, 2007). Expressing *ZmXTH1* in Arabidopsis showed alterations in the cellulose content (Genovesi *et al.*, 2008). In this study, we found that *XTH30* affected the cellulose content independent of modulating the expression of cellulose biosynthesis genes (*CesA1*, *CesA3*, *CesA6*) in response to salt stress (Fig. 6; Supplementary Fig. S12). It is possible that XTH30 somehow directly affects the synthesis/deposition of the cellulose at the plasma membrane in response to salt stress. Cellulose microfibrils are typically transversely organized and can align with cortical microtubules that are tethered to the plasma membrane (Park and Cosgrove, 2015). Microtubule depolymerization and reorganization are believed to be essential for plant survival under salt stress (Wang *et al.*, 2011; Zhang *et al.*, 2012; Dou *et al.*, 2018). *XTH30* affected the cortical microtubule depolymerization in response to salt stress (Fig. 7), which contradicted the view that microtubules mass was inversely correlated with the cellulose crystallinity and CSC velocity (Fujita *et al.*, 2011). However, there are also some studies indicating that inhibiting cellulose synthase activity with isoxaben could influence microtubule organization (Paredez *et al.*, 2008; Scheible *et al.*, 2011). XyG side chains in the xyloglucan xylosyltransferase mutant *xxt* affected cellulose synthase activity and cellulose content in primary cell walls, and disrupted microtubule stability (Xiao *et al.*, 2016).

Interestingly, knock-out mutations of *XTH30* led to lower Na$^+$ accumulation in shoots (Supplementary Fig. S9) and showed similar Na$^+$ accumulation in roots compared with the wild type, which suggests that XTH30 affected Na$^+$ transportation from root to shoot. Based on the lower Na$^+$ content and higher antioxidant defense ability, knock-out mutations of *XTH30* led to a lower level of H$_2$O$_2$ than that of the wild type under salt stress (Supplementary Figs S10, S11), which alleviated the damage of salt stress to plants. The mechanism needs to be further explored.

Thus, our findings suggest that the modified XyG side chain detected in *xth30* mutants potentially affects cellulose synthesis and cortical microtubule stability through its effects on the interactions with components of the cell wall under salt stress (Supplementary Fig. S13).

## Supplementary data

Supplementary data are available at *JXB* online.

Fig. S1. Summary of T-DNA lines used in this study.

Fig. S2. The expression of *XTH30* in wild type, *xth30-1*, and complementation of *XTH30* in *xth30-1*.

Fig. S3. The expression of *XTH30* in wild type and *XTH30* overexpressors.

Fig. S4. Sensitivity of hydroponically grown seedlings of *xth30* mutants and wild type to salt stress.

Fig. S5. *XTH30* does not affect the tolerance to heavy metal stress (Zn$^{2+}$ and Cd$^{2+}$) and ABA.

Fig. S6. *xth30* mutants are resistant to Na$^+$ and Li$^+$.

Fig. S7. *XTH30* does not affect the germination of seeds exposed to salt stress.

Fig. S8. The phenotypes of wild type and *xth30* mutants.

Fig. S9. Effect of *XTH30* on Na$^+$ accumulation in hydroponically grown seedlings exposed to salt stress.

Fig. S10. Accumulation of H$_2$O$_2$ in wild-type and *xth30* mutant seedlings.

Fig. S11. Effect of *XTH30* on the activities of antioxidant enzymes exposed to salt stress.

Fig. S12. The effect of *XTH30* on the expressions of *CesA1*, *CesA3*, and *CesA6* in response to salt stress.

Fig. S13. A potential model for XTH30 regulation in salt stress responses.

Table S1. Primer sequences used in this study.

## Accession numbers

## Acknowledgements

# References

**Ben Rejeb K, Lefebvre-De Vos D, Le Disquet I, Leprince AS, Bordenave M, Maldiney R, Jdey A, Abdelly C, Savouré A.** 2015. Hydrogen peroxide produced by NADPH oxidases increases proline accumulation during salt or mannitol stress in *Arabidopsis thaliana*. New Phytologist **208**, 1138–1148.

**Chen Z, Hong X, Zhang H, Wang Y, Li X, Zhu JK, Gong Z.** 2005. Disruption of the cellulose synthase gene, *AtCesA8/IRX1*, enhances drought and osmotic stress tolerance in Arabidopsis. The Plant Journal **43**, 273–283.

**Cho SK, Kim JE, Park JA, Eom TJ, Kim WT.** 2006. Constitutive expression of abiotic stress-inducible hot pepper *CaXTH3*, which encodes a xyloglucan endotransglucosylase/hydrolase homolog, improves drought and salt tolerance in transgenic *Arabidopsis* plants. FEBS Letters **580**, 3136–3144.

**Choi JY, Seo YS, Kim SJ, Kim WT, Shin JS.** 2011. Constitutive expression of *CaXTH3*, a hot pepper xyloglucan endotransglucosylase/hydrolase, enhanced tolerance to salt and drought stresses without phenotypic defects in tomato plants (*Solanum lycopersicum* cv. Dotaerang). Plant Cell Reports **30**, 867–877.

**Cosgrove DJ.** 2005. Growth of the plant cell wall. Nature Reviews. Molecular Cell Biology **6**, 850–861.

**Cosgrove DJ.** 2015. Plant expansins: diversity and interactions with plant cell walls. Current Opinion in Plant Biology **25**, 162–172.

**Dou L, He K, Higaki T, Wang X, Mao T.** 2018. Ethylene signaling modulates cortical microtubule reassembly in response to salt stress. Plant Physiology **176**, 2071–2081.

**Endler A, Kesten C, Schneider R, Zhang Y, Ivakov A, Froehlich A, Funke N, Persson S.** 2015. A mechanism for sustained cellulose synthesis during salt stress. Cell **162**, 1353–1364.

**Fang L, Ishikawa T, Rennie EA, et al.** 2016. Loss of inositol phosphorylceramide sphingolipid mannosylation induces plant immune responses and reduces cellulose content in *Arabidopsis*. The Plant Cell **28**, 2991–3004.

**Fry SC, Aldington S, Hetherington PR, Aitken J.** 1993. Oligosaccharides as signals and substrates in the plant cell wall. Plant Physiology **103**, 1–5.

**Fujita M, Himmelspach R, Hocart CH, Williamson RE, Mansfield SD, Wasteneys GO.** 2011. Cortical microtubules optimize cell-wall crystallinity to drive unidirectional growth in Arabidopsis. The Plant Journal **66**, 915–928.

**Genovesi V, Fornalé S, Fry SC, et al.** 2008. ZmXTH1, a new xyloglucan endotransglucosylase/hydrolase in maize, affects cell wall structure and composition in *Arabidopsis thaliana*. Journal of Experimental Botany **59**, 875–889.

**Gille S, de Souza A, Xiong G, Benz M, Cheng K, Schultink A, Reca IB, Pauly M.** 2011. O-Acetylation of *Arabidopsis* hemicellulose xyloglucan requires AXY4 or AXY4L, proteins with a TBL and DUF231 domain. The Plant Cell **23**, 4041–4053.

**Han Y, Wang W, Sun J, et al.** 2013. *Populus euphratica* XTH overexpression enhances salinity tolerance by the development of leaf succulence in transgenic tobacco plants. Journal of Experimental Botany **64**, 4225–4238.

**Hayashi T, Kaida R.** 2011. Functions of xyloglucan in plant cells. Molecular Plant **4**, 17–24.

**Hayashi T, Kaida R, Kaku T, Baba K.** 2010. Loosening xyloglucan prevents tensile stress in tree stem bending but accelerates the enzymatic degradation of cellulose. Russian Journal of Plant Physiology **57**, 316–320.

**Hayashi T, Wong YS, Maclachlan G.** 1984. Pea xyloglucan and cellulose: II. Hydrolysis by pea endo-1,4-β-glucanases. Plant Physiology **75**, 605–610.

**Huang XS, Wang W, Zhang Q, Liu JH.** 2013. A basic helix-loop-helix transcription factor, *PtrbHLH*, of *Poncirus trifoliata* confers cold tolerance and modulates peroxidase-mediated scavenging of hydrogen peroxide. Plant Physiology **162**, 1178–1194.

**Julkowska MM, Testerink C.** 2015. Tuning plant signaling and growth to survive salt. Trends in Plant Science **20**, 586–594.

**Kong Y, Peña MJ, Renna L, et al.** 2015. Galactose-depleted xyloglucan is dysfunctional and leads to dwarfism in Arabidopsis. Plant Physiology **167**, 1296–1306.

**Kooiman P.** 1960. A method for the determination of amyloid in plant seeds. Recueil des Travaux Chimiques des Pays-Bas **79**, 675–678.

**Kurasawa K, Matsui A, Yokoyama R, Kuriyama T, Yoshizumi T, Matsui M, Suwabe K, Watanabe M, Nishitani K.** 2009. The *AtXTH28* gene, a xyloglucan endotransglucosylase/hydrolase, is involved in automatic self-pollination in *Arabidopsis thaliana*. Plant & Cell Physiology **50**, 413–422.

**Labavitch JM, Ray PM.** 1974. Turnover of cell wall polysaccharides in elongating pea stem segments. Plant Physiology **53**, 669–673.

**Lee K, Lee HG, Yoon S, Kim HU, Seo PJ.** 2015. The Arabidopsis MYB96 transcription factor is a positive regulator of *ABSCISIC ACID-INSENSITIVE4* in the control of seed germination. Plant Physiology **168**, 677–689.

**Lei L, Zhang T, Strasser R, et al.** 2014. The *jiaoyao1* mutant is an allele of *korrigan1* that abolishes endoglucanase activity and affects the organization of both cellulose microfibrils and microtubules in *Arabidopsis*. The Plant Cell **26**, 2601–2616.

**Lerouxel O, Choo TS, Séveno M, Usadel B, Faye L, Lerouge P, Pauly M.** 2002. Rapid structural phenotyping of plant cell wall mutants by enzymatic oligosaccharide fingerprinting. Plant Physiology **130**, 1754–1763.

**Li W, Guan Q, Wang ZY, Wang Y, Zhu J.** 2013. A bi-functional xyloglucan galactosyltransferase is an indispensable salt stress tolerance determinant in *Arabidopsis*. Molecular Plant **6**, 1344–1354.

**Liu YB, Lu SM, Zhang JF, Liu S, Lu YT.** 2007. A xyloglucan endotransglucosylase/hydrolase involves in growth of primary root and alters the deposition of cellulose in *Arabidopsis*. Planta **226**, 1547–1560.

**Ma L, Zhang H, Sun L, Jiao Y, Zhang G, Miao C, Hao F.** 2012. NADPH oxidase AtrbohD and AtrbohF function in ROS-dependent regulation of Na$^+$/K$^+$ homeostasis in *Arabidopsis* under salt stress. Journal of Experimental Botany **63**, 305–317.

**Matsui A, Yokoyama R, Seki M, Ito T, Shinozaki K, Takahashi T, Komeda Y, Nishitani K.** 2005. AtXTH27 plays an essential role in cell wall modification during the development of tracheary elements. The Plant Journal **42**, 525–534.

**Munns R, Tester M.** 2008. Mechanisms of salinity tolerance. Annual Review of Plant Biology **59**, 651–681.

**Mutwil M, Debolt S, Persson S.** 2008. Cellulose synthesis: a complex complex. Current Opinion in Plant Biology **11**, 252–257.

**Nelson BK, Cai X, Nebenführ A.** 2007. A multicolored set of in vivo organelle markers for co-localization studies in *Arabidopsis* and other plants. The Plant Journal **51**, 1126–1136.

**Nishikubo N, Takahashi J, Roos AA, Derba-Maceluch M, Piens K, Brumer H, Teeri TT, Stålbrand H, Mellerowicz EJ.** 2011. Xyloglucan endo-transglycosylase-mediated xyloglucan rearrangements in developing wood of hybrid aspen. Plant Physiology **155**, 399–413.

**Nishitani K, Tominaga R.** 1992. Endo-xyloglucan transferase, a novel class of glycosyltransferase that catalyzes transfer of a segment of xyloglucan molecule to another xyloglucan molecule. The Journal of Biological Chemistry **267**, 21058–21064.

**Paredez AR, Persson S, Ehrhardt DW, Somerville CR.** 2008. Genetic evidence that cellulose synthase activity influences microtubule cortical array organization. Plant Physiology **147**, 1723–1734.

**Park YB, Cosgrove DJ.** 2015. Xyloglucan and its interactions with other components of the growing cell wall. Plant & Cell Physiology **56**, 180–194.

**Pauly M, Keegstra K.** 2016. Biosynthesis of the plant cell wall matrix polysaccharide xyloglucan. Annual Review of Plant Biology **67**, 235–259.

**Refrégier G, Pelletier S, Jaillard D, Höfte H.** 2004. Interaction between wall deposition and cell elongation in dark-grown hypocotyl cells in Arabidopsis. Plant Physiology **135**, 959–968.

**Scheible WR, Eshed R, Richmond T, Delmer D, Somerville C.** 2011. Modifications of cellulose synthase confer resistance to isoxaben and thiazolidinone herbicides in *Arabidopsis ixr1* mutants. Proceedings of the National Academy of Sciences, USA **98**, 10079–10084.

**Scheller HV, Ulvskov P.** 2010. Hemicelluloses. Annual Review of Plant Biology **61**, 263–289.

**Sechet J, Frey A, Effroy-Cuzzi D, et al.** 2016. Xyloglucan metabolism differentially impacts the cell wall characteristics of the endosperm and embryo during Arabidopsis seed germination. Plant Physiology **170**, 1367–1380.

**Shi H, Ishitani M, Kim C, Zhu JK.** 2000. The *Arabidopsis thaliana* salt tolerance gene *SOS1* encodes a putative Na⁺/H⁺ antiporter. Proceedings of the National Academy of Sciences, USA **97**, 6896–6901.

**Shi YZ, Zhu XF, Miller JG, Gregson T, Zheng SJ, Fry SC.** 2015. Distinct catalytic capacities of two aluminium-repressed *Arabidopsis thaliana* xyloglucan endotransglucosylase/hydrolases, XTH15 and XTH31, heterologously produced in *Pichia*. Phytochemistry **112**, 160–169.

**Strohmeier M, Hrmova M, Fischer M, Harvey AJ, Fincher GB, Pleiss J.** 2004. Molecular modeling of family GH16 glycoside hydrolases: potential roles for xyloglucan transglucosylases/hydrolases in cell wall modification in the Poaceae. Protein Science **13**, 3200–3213.

**Tamura K, Shimada T, Kondo M, Nishimura M, Hara-Nishimura I.** 2005. KATAMARI1/MURUS3 is a novel Golgi membrane protein that is required for endomembrane organization in Arabidopsis. The Plant Cell **17**, 1764–1776.

**Tenhaken R.** 2014. Cell wall remodeling under abiotic stress. Frontiers in Plant Science **5**, 771.

**Thompson JE, Fry SC.** 2001. Restructuring of wall-bound xyloglucan by transglycosylation in living plant cells. The Plant Journal **26**, 23–34.

**Vuttipongchaikij S, Brocklehurst D, Steele-King C, Ashford DA, Gomez LD, McQueen-Mason SJ.** 2012. Arabidopsis GT34 family contains five xyloglucan α-1,6-xylosyltransferases. New Phytologist **195**, 585–595.

**Wang R, Jing W, Xiao L, Jin Y, Shen L, Zhang W.** 2015. The rice high-affinity potassium Transporter1;1 is involved in salt tolerance and regulated by an MYB-type transcription factor. Plant Physiology **168**, 1076–1090.

**Wang S, Kurepa J, Hashimoto T, Smalle JA.** 2011. Salt stress-induced disassembly of *Arabidopsis* cortical microtubule arrays involves 26S proteasome-dependent degradation of SPIRAL1. The Plant Cell **23**, 3412–3427.

**Wang T, McFarlane HE, Persson S.** 2016. The impact of abiotic factors on cellulose synthesis. Journal of Experimental Botany **67**, 543–552.

**Xiao C, Zhang T, Zheng Y, Cosgrove DJ, Anderson CT.** 2016. Xyloglucan deficiency disrupts microtubule stability and cellulose biosynthesis in Arabidopsis, altering cell growth and morphogenesis. Plant Physiology **170**, 234–249.

**Xu Z, Wang M, Shi D, Zhou G, Niu T, Hahn MG, O'Neill MA, Kong Y.** 2017. DGE-seq analysis of MUR3-related *Arabidopsis* mutants provides insight into how dysfunctional xyloglucan affects cell elongation. Plant Science **258**, 156–169.

**Yan J, Guan L, Sun Y, Zhu Y, Liu L, Lu R, Jiang M, Tan M, Zhang A.** 2015. Calcium and ZmCCaMK are involved in brassinosteroid-induced antioxidant defense in maize leaves. Plant & Cell Physiology **56**, 883–896.

**Yokoyama R, Nishitani K.** 2001. A comprehensive expression analysis of all members of a gene family encoding cell-wall enzymes allowed us to predict *cis*-regulatory regions involved in cell-wall construction in specific organs of Arabidopsis. Plant & Cell Physiology **42**, 1025–1033.

**Yokoyama R, Rose JK, Nishitani K.** 2004. A surprising diversity and abundance of xyloglucan endotransglucosylase/hydrolases in rice. Classification and expression analysis. Plant Physiology **134**, 1088–1099.

**Zhang Q, Lin F, Mao T, Nie J, Yan M, Yuan M, Zhang W.** 2012. Phosphatidic acid regulates microtubule organization by interacting with MAP65-1 in response to salt stress in *Arabidopsis*. The Plant Cell **24**, 4555–4576.

**Zhang SS, Sun L, Dong X, Lu SJ, Tian W, Liu JX.** 2016*a*. Cellulose synthesis genes *CESA6* and *CSI1* are important for salt stress tolerance in *Arabidopsis*. Journal of Integrative Plant Biology **58**, 623–626.

**Zhang Y, Nikolovski N, Sorieul M, et al.** 2016*b*. Golgi-localized STELLO proteins regulate the assembly and trafficking of cellulose synthase complexes in *Arabidopsis*. Nature Communications **7**, 11656.

**Zhu JK.** 2002. Salt and drought stress signal transduction in plants. Annual Review of Plant Biology **53**, 247–273.

**Zhu JK.** 2016. Abiotic stress signaling and responses in plants. Cell **167**, 313–324.

**Zhu XF, Shi YZ, Lei GJ, et al.** 2012. *XTH31*, encoding an in vitro XEH/XET-active enzyme, regulates aluminum sensitivity by modulating in vivo XET action, cell wall xyloglucan content, and aluminum binding capacity in *Arabidopsis*. The Plant Cell **24**, 4731–4747.

**Zhu Y, Yan J, Liu W, et al.** 2016. Phosphorylation of a NAC transcription factor by a calcium/calmodulin-dependent protein kinase regulates abscisic acid-induced antioxidant defense in maize. Plant Physiology **171**, 1651–1664.